EDGE ARTICLE

Check for updates

Metal *vs.* ligand protonation and the alleged proton-shuttling role of the azadithiolate ligand in catalytic H$_2$ formation with FeFe hydrogenase model complexes†

Alexander Aster, [iD] ‡ Shihuai Wang, Mohammad Mirmohades, Charlène Esmieu,§ Gustav Berggren, [iD] Leif Hammarström and Reiner Lomoth [iD] *

Electron and proton transfer reactions of diiron complexes [Fe$_2$adt(CO)$_6$] (**1**) and [Fe$_2$adt(CO)$_4$(PMe$_3$)$_2$] (**4**), with the biomimetic azadithiolate (adt) bridging ligand, have been investigated by real-time IR- and UV-vis-spectroscopic observation to elucidate the role of the adt-N as a potential proton shuttle in catalytic H$_2$ formation. Protonation of the one-electron reduced complex, **1**$^-$, occurs on the adt-N yielding **1H** and the same species is obtained by one-electron reduction of **1H**$^+$. The preference for ligand *vs.* metal protonation in the Fe$_{(I,0)}$ state is presumably kinetic but no evidence for tautomerization of **1H** to the hydride **1Hy** was observed. This shows that the adt ligand does not work as a proton relay in the formation of hydride intermediates in the reduced catalyst. A hydride intermediate **1HHy**$^+$ is formed only by protonation of **1H** with stronger acid. Adt protonation results in reduction of the catalyst at much less negative potential, but subsequent protonation of the metal centers is not slowed down, as would be expected according to the decrease in basicity. Thus, the adtH$^+$ complex retains a high turnover frequency at the lowered overpotential. Instead of proton shuttling, we propose that this gain in catalytic performance compared to the propyldithiolate analogue might be rationalized in terms of lower reorganization energy for hydride formation with bulk acid upon adt protonation.

Introduction

Proton binding sites in the second coordination sphere of catalytic metal centres are widely considered as an important design principle for facilitating proton coupled electron transfer in molecular catalysts for *e.g.* water splitting,[1–5] H$_2$ formation and activation[6–12] or CO$_2$ reduction.[13–21] For the directed design of synthetic catalysts it is, however, important to note that improvements to catalytic performance (TOF, overpotential) brought about by basic sites in the second coordination sphere are not necessarily arising from a proton relay activity. Instead, the modulation of redox and acid/base properties of the metal centre upon changes in protonation state in the second coordination sphere may be the actual origin of improved catalytic performance.[14–17]

Regarding catalysts for H$_2$ formation, the N$_2$P$_2$ ligands introduced by DuBois and co-workers,[6,7,12] and the azadiolate (adt) bridging ligand in diiron complexes of the general formula Fe$_2$adt(CO)$_4$X$_2$ (X = *e.g.* CO, R$_3$P) modelled after the FeFe-Hase active site,[9,22–24] are prominent examples of ligand motifs with basic sites in the second coordination sphere. The amine function of the adt ligand is believed to assist enzymatic H$_2$ formation and activation by shuttling of protons to or from the distal iron centre of the active site where the crucial terminal hydride intermediate is formed (Scheme 1a).[25,26] A similar role of the adt ligand in catalysis by the synthetic models considered here seems less likely given the preferred bridging coordination of the hydride (Scheme 1b).[23] The superior catalytic performance of Fe$_2$(adt)(CO)$_6$, **1**, over its propyldithiolate (pdt)

Department of Chemistry-Ångström Laboratory, Uppsala University, Box 523, SE-751 20 Uppsala, Sweden. E-mail: reiner.lomoth@kemi.uu.se

† Electronic supplementary information (ESI) available: Experimental details, UV-vis transient absorption spectra of **1**$^-$ and **1H**. See DOI: 10.1039/c9sc00876d

‡ Present address: Department of Physical Chemistry, University of Geneva, 30 quai Ernest Ansermet, CH-1211 Geneva, Switzerland.

§ Present address: CNRS, LCC (Laboratoire de Chimie de Coordination), 205 route de Narbonne, BP 44099 31077 Toulouse cedex 4, France.
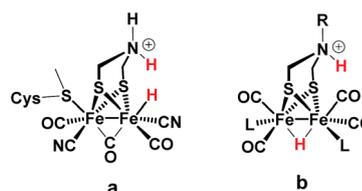
Scheme 1 FeFe Hase active site (a) and synthetic model (b) bearing a hydride and a proton.

analogue **2** in electrochemical H_2 formation has however been attributed to proton shuttling, involving specifically terminal protonation of the metal centre by tautomerization of a adt-NH^+ precursor upon one-electron reduction of the catalyst.[27] We were therefore intrigued whether the proposed role of the adt ligand as proton shuttle and the formation of terminal hydride intermediates in these model complexes could be inferred from direct spectroscopic observation. For this purpose we have combined laser flash induced reduction as well as rapid chemical reduction of the catalyst with both UV-vis and IR detection to elucidate structure and reactivity of reduced and reduced-protonated intermediates derived from **1** (ref. 28) and $Fe_2(adt)(CO)_4(PMe_3)_2$ (**4**).[29] This approach enabled us to exclude any proton shuttling role of the adt bridging ligand in catalytic H_2 formation while the kinetics of ligand and metal protonation steps suggest an alternative rationale for the improved performance.

1   2   3   4 (R=H),   4' (R=4-Br-benzyl)
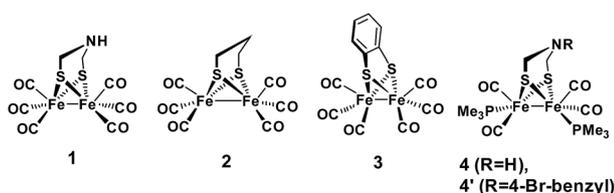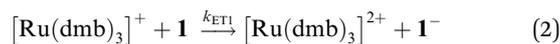
Results and discussion

Generally, complex **1** catalyses H_2 formation via an initial ET-PT sequence with weaker acids, or a PT-ET sequence when stronger acids are employed that initially protonate the adt-N with a pK_a of 8 in acetonitrile[30] (Scheme 2, potentials from ref. 27).
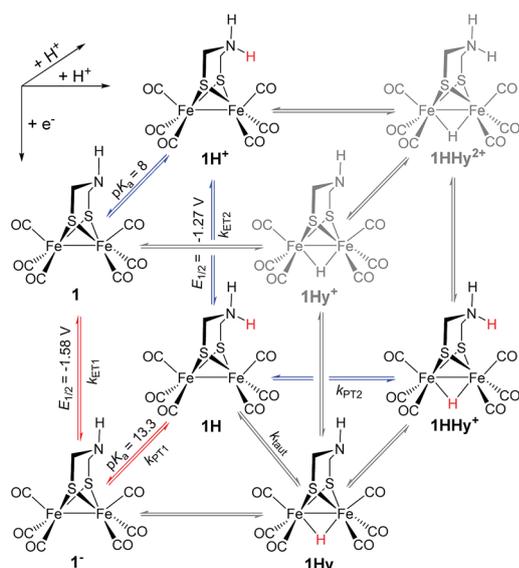
Scheme 2 Metal and ligand protonation reactions of **1** ($Fe_2(I,I)$) and **1⁻** ($Fe_2(I,0)$).

Reduction of 1

To investigate the ET-PT route, the one-electron reduced catalyst **1⁻** was obtained by rapid electron transfer from laser flash generated $[Ru(dmb)_3]^+$ according to eqn (1) and (2) ($k_{ET1} = 3 \times 10^9$ M^{-1} s^{-1}, eqn (2)). The electronic absorption bands of **1⁻** (570, 700 nm, see ESI†) and the carbonyl region of its IR spectrum (1915, 1945, 2005 cm^{-1}, Fig. 1a) resemble closely the spectra reported for the singly reduced pdt analogue **2⁻**.[31,32] The 700 nm band and the uniform shift of the three ν_{C-O} bands by 80–90 cm^{-1} towards lower wavenumbers are distinct markers of the intact $(\mu^2,\kappa^2\text{-adt})Fe_2(CO)_6$ core in the reduced complex **1⁻**, in contrast to the dissociation of a sulphur–iron bond in the reduced bdt analogue (bdt = benzene-1,2-dithiolate) **3⁻**.[33] In the absence of proton sources, decay of **1⁻** leads to complete recovery of **1** by diffusion controlled charge recombination with the electron donor radical TTF^+ ($k_{rec,1} = 6 \times 10^{10}$ M^{-1} s^{-1}, eqn (3)).

$$[Ru(dmb)_3]^{2+*} + TTF \xrightarrow{k_q} [Ru(dmb)_3]^+ + TTF^+ \quad (1)$$

$$[Ru(dmb)_3]^+ + \mathbf{1} \xrightarrow{k_{ET1}} [Ru(dmb)_3]^{2+} + \mathbf{1^-} \quad (2)$$

$$\mathbf{1^-} + TTF^+ \xrightarrow{k_{rec,1}} \mathbf{1} + TTF \quad (3)$$

Metal vs. ligand protonation of 1⁻

Protonation of the laser flash generated **1⁻** (eqn (4)) with weak acids (Cl_3CCOOH, $pK_a = 10.6$ or $ClCH_2COOH$, $pK_a = 15.3$),[34]
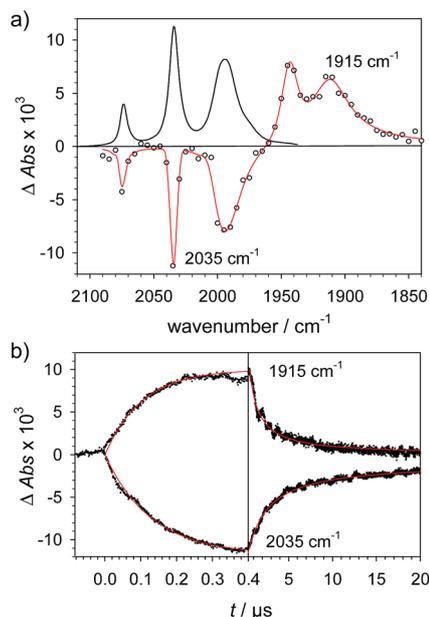
Fig. 1 (a) Transient IR spectrum 1 µs after excitation (○, ▬) and normalized IR spectrum of the starting state (▬) for the reduction of **1** (1.3 mM) by flash-quench generated $[Ru(dmb)_3]^+$ in acetonitrile. (b) Kinetic traces (···) and fits (▬) monitoring the pseudo-first order formation of **1⁻** (1915 cm^{-1}) and bleach of **1** (2035 cm^{-1}) followed by second order charge recombination with TTF^+.

which avoids protonation of the neutral parent complex, shifts all three ν_{C-O} bands by about 20 cm^{-1} to higher wavenumbers (2025, 1965 and 1935 cm^{-1}), as shown in Fig. 2. The magnitude of the shift is similar to what is observed upon protonation of the neutral parent complex with stronger acids (*cf.* Fig. 3a) and characteristic for protonation of the adt-N.[29]

$$1^- + AH \xrightarrow{k_{PT1}} 1H + A^- \qquad (4)$$

Metal protonation of 1^- is on the other hand expected to shift the carbonyl bands by about 80 cm^{-1} to higher wavenumbers. Shifts of this magnitude have been established for the bridging hydrides formed by protonation of Fe$_2$(I,I) complexes with electron donor ligands like $4'$ (ref. 35) as well as transiently generated Fe$_2$(I,0) hexacarbonyl complexes 2^- and 3^-.[32,33] Mutually cancelling shifts of the carbonyl bands upon one-electron reduction and metal protonation were further evidenced with help of complex 4 (*vide infra*). The transient IR spectrum of the protonation product hence proves that the adt ligand remains the preferred site of protonation, at least kinetically, also upon one-electron reduction of 1. This conclusion is corroborated by the UV-vis spectrum of $1H$ (ESI†), which is similar to its precursor 1^-, while metal protonation of 2^- was previously shown to cause complete bleach of its visible absorption bands that arise from transitions involving predominantly metal-based orbitals. The observed pseudo-first order rate constants for formation of $1H$ follow a linear dependence on acid concentration before becoming limited by

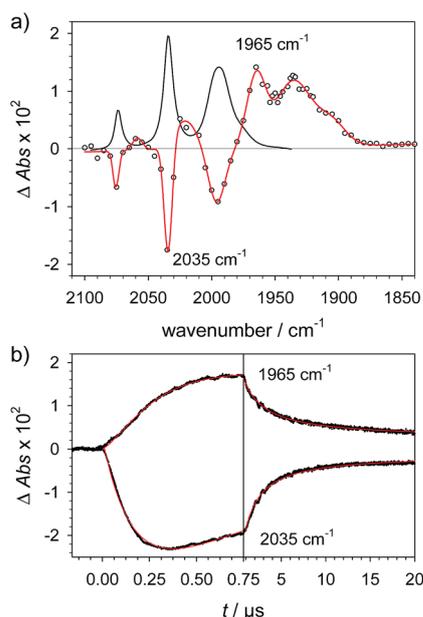Fig. 3 (a) FTIR spectra of 4 (1.5 mM) (—) in acetonitrile, $4H^+$ (—) obtained by protonation with toluenesulfonic acid (3 mM), and $4Hy^+$ (—) obtained by protonation with toluenesulfonic acid (3 mM) in presence of tetrabutyl-ammonium chloride (1.5 mM) after correction of the raw spectrum (— — —) for minor contribution from $4H^+$. (b) Transient IR spectrum upon reduction of $4Hy^+$ to $4Hy$ by electron transfer from flash-quench generated [Ru(dmb)$_3$]$^+$ (O, —, 1 μs after excitation) and normalized IR spectra of $4Hy^+$ (— — —) and 4 (—).

Fig. 2 (a) Transient IR spectrum 1 μs after excitation (O, —) and normalized IR spectrum of the starting state (—) for formation of $1H$ by protonation of 1^- with Cl$_3$CCOOH (13 mM) following reduction of 1 (1.3 mM) by flash-quench generated [Ru(dmb)$_3$]$^+$ in acetonitrile. (b) Kinetic traces (⋯) and fits (—) monitoring pseudo-first order formation of $1H$ (1965 cm^{-1}) and bleach of 1 (2035 cm^{-1}) followed by second order charge recombination with TTF$^+$.

the preceding electron transfer step (ESI†). The straightforward concentration dependence excludes any complications of the protonation kinetics due to dimerization of the acetic acids that was previously found to result in quadratic concentration dependence corresponding to an increase in effective acid strength.[36] Interestingly, protonation of 1^-, which occurs unambiguously at the adt-N, proceeds remarkably slowly with bimolecular rate constants k_{PT1} of 4×10^8 M^{-1} s^{-1} and 2×10^7 M^{-1} s^{-1} for Cl$_3$CCOOH and ClH$_2$CCOOH, respectively.

Notably, the protonation rate constant is almost two orders of magnitude below the diffusion controlled limit even for the strongly exergonic reaction with Cl$_3$CCOOH ($\Delta pK_a = 3$). This is quite untypical for protonation of an amine base and indicative of significant reorganization associated with ligand protonation.

Spectral comparison against the one-electron reduced hydride 4Hy

The above assignment of the protonation reaction to ligand protonation builds to a large extent on the general notion of nearly perfectly cancelling shifts in carbonyl frequencies caused by one-electron reduction and formation of a bridging hydride. This expectation could previously only be supported by the vanishing transient absorption observed upon protonation of complexes 2^- and 3^-.[32,33] Here, these assignments could be

eventually verified by the positive observation of a one-electron reduced hydride **4Hy** by laser flash induced reduction of hydride complex **4Hy⁺**. The latter can be obtained by the Cl⁻-catalysed protonation of **4** that yields the thermodynamically stable hydride instead of the kinetically preferred ligand protonated **4H⁺** in analogy to the previously reported behaviour of **4′**.[37] Upon one electron reduction of **4Hy⁺** the carbonyl bands of the product **4Hy** coincide almost perfectly with those of the parent complex **4** (Fig. 3) verifying the close spectral resemblance of the diiron carbonyl complexes and their bridging hydride derivatives in the Fe₂(ɪ,0) oxidation state.

Probing possible tautomerization of 1H

According to the above arguments, also formation of a possibly more stable hydride **1Hy** by tautomerization (5) should lead to complete decay of all transient absorption given the predictable spectral similarity between **1** and **1Hy**.

$$\mathbf{1H} \xrightarrow{k_{\text{taut}}} \mathbf{1Hy} \qquad (5)$$

While the expected spectral changes are the same as for charge recombination between **1H** and TTF⁺ (6), tautomerization should nevertheless accelerate the decay of **1H** if it proceeds with a rate that is at least comparable to charge recombination (6).

$$\mathbf{1H} + \text{TTF}^+ \xrightarrow{k_{\text{rec,2}}} \mathbf{1} + \text{TTF} + \text{H}^+ \qquad (6)$$

In flash photolysis experiments, **1H** decays with second order kinetics on a time scale of about 10 μs in transient IR and about 100 μs with the lower transient concentrations in UV-vis experiments. These time scales are typical for diffusion controlled recombination ($k_{\text{rec,2}} = 1.5 \times 10^{10}$ M⁻¹ s⁻¹) and put an upper limit on the order of 10^4 s⁻¹ on the rate constant of a possibly competing tautomerization reaction.

As a turnover frequency (TOF) of 10^3 to 10^4 s⁻¹ has been proposed from electrocatalytic experiments ($\log(k_{\text{cat}}/\text{s}^{-1}) = 3.9$ and 2.6 for 6 mM Cl₃CCOOH and ClH₂CCOOH, respectively),[27] we wanted to probe the reactivity of **1H** on a longer time scale than 100 μs. Thus, **1H⁺** was chemically reduced by cobaltocene in IR stopped flow experiments (rapid-scan FTIR). **1H⁺** was obtained by addition of two equivalents of 2,5-dichlorobenzenesulfonic acid (Cl₂BSA, pK_a = 6.7)[34] to warrant quantitative protonation of **1**. Reduction to **1H** occurred on a shorter time scale than the time resolution of the experiment. Importantly, **1H** was observed for several seconds (Fig. 4). Its decay with a lifetime of 1.3 s yields a product spectrum that can be assigned to the parent complex **1** or the tautomerization product **1Hy** given the expected similarity of their spectra. The former could be generated by catalytic turnover that leads to depletion of acid and therefore regenerates unreduced, unprotonated catalyst. Whether the slow decay of **1H** is predominantly due to turnover or tautomerization cannot be discriminated but the observed lifetime demonstrates in either case that the rate constant for tautomerization, if this occurs at all, has to be smaller than 1 s⁻¹. We note that tautomerization
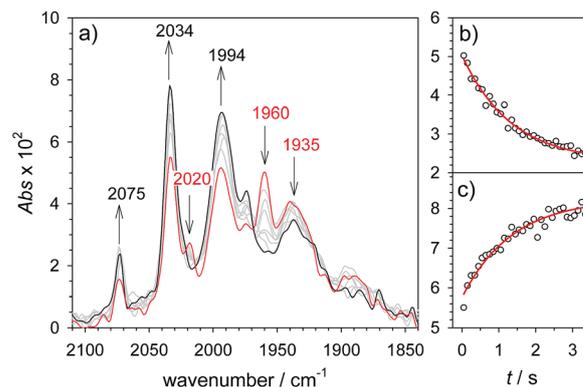

Fig. 4 Rapid scan FTIR spectra in acetonitrile between 50 ms (━) and 3 s (━) after after mixing of **1H⁺** (1.3 mM **1**, 2.6 mM Cl₂BSA) with cobaltocene (20 mM) (a) and kinetic traces (○) with exponential fits (━) monitoring decay of **1H** at 1960 cm⁻¹ (b) and formation of **1** at 2034 cm⁻¹ (c).

would be an intramolecular process that is independent on external conditions, such as identity and concentration of acid and the method of reduction (chemical or electrochemical).

Reduction and subsequent protonation of 1H⁺

Alternative formation of **1H** *via* the PT-ET route was studied by laser-flash induced reduction of **1H⁺** (7).

$$\left[\text{Ru(dmb)}_3\right]^+ + \mathbf{1H}^+ \xrightarrow{k_{\text{ET2}}} \left[\text{Ru(dmb)}_3\right]^{2+} + \mathbf{1H} \qquad (7)$$

1H⁺ was obtained by protonation of **1** with Cl₂BSA that shifts the IR peaks by about 20 cm⁻¹ to higher wavenumbers (2090, 2051 and 2015 cm⁻¹).[29] The transient IR absorption spectrum after reduction of **1H⁺** (Fig. 5) shows the bleaching of all three $\nu_{\text{C-O}}$ peaks of **1H⁺** together with the same product absorption peaks previously attributed to **1H** (2025, 1965, 1935 cm⁻¹). While the ET-PT and PT-ET sequences lead expectedly to the same product **1H**, its decay is much faster when generated in presence of the stronger acid required for the initial ligand protonation. The accelerated decay of **1H** (Fig. 5) without appearance of new transient signals can be assigned to its metal protonation yielding **1HHy⁺** (8).

$$\mathbf{1H} + \text{AH} \xrightarrow{k_{\text{PT2}}} \mathbf{1HHy}^+ + \text{A}^- \qquad (8)$$
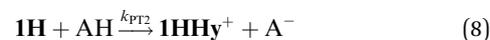
This assignment is based on the expected IR absorption of **1HHy⁺** that is likely to cancel the bleach of absorption from the starting material **1H⁺** as previously found for hydrides **2Hy** and **3Hy**.[32,33] Protonation is also manifested in a slower charge recombination of **1HHy⁺** with TTF⁺ (ESI†). Kinetic analysis of both **1H** and TTF⁺ signals results in a protonation rate constant of $k_{\text{PT2}} = 6 \times 10^7$ M⁻¹ s⁻¹ (see ESI†). The analysis eliminates the possible effect of accelerated recombination with accumulated TTF⁺ in the presence of acid. With a rate constant of 6×10^7 M⁻¹ s⁻¹ formation of the hydride **1HHy⁺** by metal protonation of **1H** with Cl₂BSA (pK_a 6.7)[34] occurs about as fast as metal protonation of the pdt analogue **2⁻** (7×10^7 M⁻¹ s⁻¹)[32] by TsOH
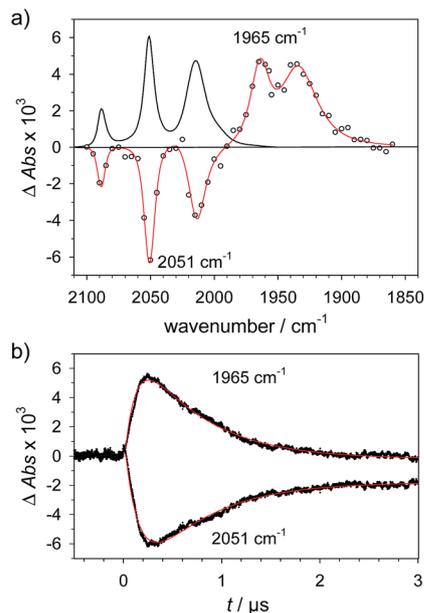
Fig. 5 (a) Transient IR spectrum 0.3 μs after excitation (○, ▬) and normalized IR spectrum of the starting state (▬) for formation of **1H** by reduction of **1H$^+$** (obtained by protonation of **1** with 2.6 mM Cl$_2$BSA) with flash-quench generated [Ru(dmb)$_3$]$^+$ in acetonitrile. (b) Kinetic traces (⋯) and fits (▬) monitoring pseudo-first order formation of **1H** (1965 cm^{-1}) and bleach of **1H$^+$** (2051 cm^{-1}) followed by pseudo-first order decay of **1H** by protonation with Cl$_2$BSA and charge recombination with TTF$^+$.

(pK_a 8–8.7).[34] Both complexes are in the same Fe$_2$(ɪ,0) oxidation state but the pK_a of the hydride should drop by about 5 units according to a shift of +330 mV in reduction potential for the **1H$^+$/1H** couple compared to **1/1$^-$** or **2/2$^-$**. Protonation of **1H**, even by the stronger Cl$_2$BSA, is therefore thermodynamically less favourable than protonation of **2$^-$** by TsOH, with ΔpK_a lowered by about 3 for the former reaction. Applying the free energy relationship (Brønsted coefficient of 0.4) established for protonation of **2$^-$**,[32] the protonation of **1H** to **1HHy$^+$** is hence one to two orders of magnitude faster than expected for protonation of its pdt analogue **2$^-$** with the same driving force. Intrinsically faster protonation of the adt-protonated **1H** would prevent this step from becoming rate limiting when reducing weaker acids. Below, we discuss the possible origin of this favourable effect.

Implications for (electro)catalytic H$_2$ formation

From previous electrochemical experiments comparing **1** and **2** it has been concluded that catalytic H$_2$ formation from the same acids proceeds with similar second order catalytic rate constants despite the lower overpotential arising from the easier reduction of adt-protonated catalyst.[27] Undiminished reactivity towards protonation despite the lowered driving force would imply that **1** breaks the usual scaling relation between overpotential and rate,[38] an effect that has been attributed to the proton shuttling role of the adt[27] ligand. By putting an upper limit of 1 s^{-1} on the first order rate constant for intramolecular

tautomerization, our results exclude however that a mechanism involving hydride formation by proton shuttling at the Fe$_2$(0,ɪ) redox level could under any conditions result in the reported pseudo-first order catalytic rate constant on the order of 10^3 to 10^4 s^{-1}, as previously proposed.[27] It is important to note that the reported kinetics refer to the first catalytic wave (−1.4 V) that has been attributed to mechanisms where the hydride is formed prior to the second electron transfer, *i.e.* a CECE sequence with stronger acids or an ECCE sequence with weak acids. Therefore, possible formation of the hydride *via* tautomerization at the Fe$_2$(0,0) redox level (**1H$^-$** → **1Hy$^-$**) cannot explain the superior catalytic performance of the adt complex.

An alternative advantage of the adt ligand might instead arise from the lowered barrier for hydride formation due to the structural changes at the iron core induced by the preceding ligand protonation. This notion would be in line with the relative sluggishness of the latter reaction (see above) and is corroborated by structural data that has been previously obtained from EXAFS spectra[39] of ligand- and metal-protonated states of the related Fe$_2$(ɪ,ɪ) complex **4′**.¶[37] Specifically, protonation of the adt ligand in **4′** results in an elongated Fe–Fe bond distance in **4′H$^+$** that is close to the distance found in the bridging hydride **4′HHy^{2+}**. Formation of the hydride from the ligand protonated complex requires hence much less reorganization of this coordinate than formation of hydride **4′Hy$^+$** from **4′**.

Generally, a proton shuttling ligand could accelerate not only the formation of the hydride intermediate but also its subsequent coupling with a proton. In case of adt complex **1**, with its bridging hydride intermediate, neither of the two steps is, however, likely to involve the adt-N, for steric reasons. In contrast to the terminal hydride of the enzyme active site, the hydride is bridging in the model complex (*cf.* Scheme 1), as evidenced by the conserved symmetry shown by the IR spectra, and the absence of a bridging CO IR band. The superior catalytic performance of **1** over its pdt analogue **2** is instead attributed to the observed acceleration of hydride formation with bulk acid as described above.

Conclusions

In summary, we could demonstrate by real-time spectroscopic observation that the initial protonation of hydrogenase model complex **1**, also in its one-electron reduced Fe$_2$(ɪ,0) state **1$^-$**, occurs on the adt ligand rather than the Fe$_2$ core. The same ligand protonated intermediate **1H** was alternatively generated by one-electron reduction of **1H$^+$** and no evidence for tautomerization of **1H** to a potentially more stable hydride **1Hy** was observed in either case. **1H** was stable on the time scale of 1 s, which shows that intramolecular proton shuttling cannot be responsible for the reported catalytic TOFs of 10^3 to 10^4 s^{-1}.[27] For catalytic H$_2$ generation from weak acids this implies that no hydride intermediate is formed on the Fe$_2$(ɪ,0) level; instead, hydride formation may occur after further reduction, by direct protonation in the Fe$_2$(0,0) state. Only with strong acids a doubly protonated intermediate **1HHy$^+$** is formed in the Fe$_2$(ɪ,0) state, by direct metal protonation of **1H**, not by ligand

protonation of a hydride precursor. Generally, it can therefore be concluded that, in contrast to the enzymatic reaction, the adt ligand of model complex **1** has no proton relay function that enables rapid formation of the bridging hydride intermediates on the $Fe_2(I,0)$ level. The protonation kinetics reveal however an exceptionally high barrier for protonation of the adt ligand that we suggest in turn may lower the barrier for hydride formation, presumably due to rearrangements of the metal core upon ligand protonation. In this way the basic site in the second coordination sphere might allow the catalyst to overcome the usual trade-off between overpotential and rate without invoking any proton-shuttling role.

Conflicts of interest

There are no conflicts to declare.

Acknowledgements

Notes and references

¶ Protonation kinetics of the phosphine complexes **4** (ref. 29) and **4′** (ref. 37) have so far been studied only in the $Fe_2(I,I)$ state where hydride formation is extremely slow.

1 D. K. Dogutan, R. McGuire and D. G. Nocera, *J. Am. Chem. Soc.*, 2011, **133**, 9178–9180.

2 J. L. Boyer, D. E. Polyansky, D. J. Szalda, R. F. Zong, R. P. Thummel and E. Fujita, *Angew. Chem., Int. Ed.*, 2011, **50**, 12600–12604.

3 Y. M. Badiei, D. E. Polyansky, J. T. Muckerman, D. J. Szalda, R. Haberdar, R. Zong, R. P. Thummel and E. Fujita, *Inorg. Chem.*, 2013, **52**, 8845–8850.

4 W. A. Hoffert, M. T. Mock, A. M. Appel and J. Y. Yang, *Eur. J. Inorg. Chem.*, 2013, **2013**, 3846–3857.

5 H. L. Sun, Y. Z. Han, H. T. Lei, M. X. Chen and R. Cao, *Chem. Commun.*, 2017, **53**, 6195–6198.

6 M. R. DuBois and D. L. DuBois, *Chem. Soc. Rev.*, 2009, **38**, 62–72.

7 S. E. Smith, J. Y. Yang, D. L. DuBois and R. M. Bullock, *Angew. Chem., Int. Ed.*, 2012, **51**, 3152–3155.

8 M. O'Hagan, W. J. Shaw, S. Raugei, S. Chen, J. Y. Yang, U. J. Kilgore, D. L. DuBois and R. M. Bullock, *J. Am. Chem. Soc.*, 2011, **133**, 14301–14312.

9 T. B. Rauchfuss, *Acc. Chem. Res.*, 2015, **48**, 2107–2116.

10 P. F. Huo, C. Uyeda, J. D. Goodpaster, J. C. Peters and T. F. Miller, *ACS Catal.*, 2016, **6**, 6114–6123.

11 S. Raugei, M. L. Helm, S. Hammes-Schiffer, A. M. Appel, M. O'Hagan, E. S. Wiedner and R. M. Bullock, *Inorg. Chem.*, 2016, **55**, 445–460.

12 B. Ginovska-Pangovska, A. Dutta, M. L. Reback, J. C. Linehan and W. J. Shaw, *Acc. Chem. Res.*, 2014, **47**, 2621–2630.

13 M. R. Dubois and D. L. Dubois, *Acc. Chem. Res.*, 2009, **42**, 1974–1982.

14 J. T. Bays, N. Priyadarshani, M. S. Jeletic, E. B. Hulley, D. L. Miller, J. C. Linehan and W. J. Shaw, *ACS Catal.*, 2014, **4**, 3663–3670.

15 C. Costentin, G. Passard, M. Robert and J.-M. Savéant, *J. Am. Chem. Soc.*, 2014, **136**, 11821–11829.

16 M. L. Pegis, B. A. McKeown, N. Kumar, K. Lang, D. J. Wasylenko, X. P. Zhang, S. Raugei and J. M. Mayer, *ACS Cent. Sci.*, 2016, **2**, 850–856.

17 A. M. Lilio, M. H. Reineke, C. E. Moore, A. L. Rheingold, M. K. Takase and C. P. Kubiak, *J. Am. Chem. Soc.*, 2015, **137**, 8251–8260.

18 C. W. Machan, J. Yin, S. A. Chabolla, M. K. Gilson and C. P. Kubiak, *J. Am. Chem. Soc.*, 2016, **138**, 8184–8193.

19 S. Roy, B. Sharma, J. Peaut, P. Simon, M. Fontecave, P. D. Tran, E. Derat and V. Artero, *J. Am. Chem. Soc.*, 2017, **139**, 3685–3696.

20 W. H. Wang, J. F. Hull, J. T. Muckerman, E. Fujita and Y. Himeda, *Energy Environ. Sci.*, 2012, **5**, 7923–7926.

21 A. Chapovetsky, M. Welborn, J. M. Luna, R. Haiges, T. F. Miller and S. C. Marinescu, *ACS Cent. Sci.*, 2018, **4**, 397–404.

22 C. Tard and C. J. Pickett, *Chem. Rev.*, 2009, **109**, 2245–2274.

23 D. Schilter, J. M. Camara, M. T. Huynh, S. Hammes-Schiffer and T. B. Rauchfuss, *Chem. Rev.*, 2016, **116**, 8693–8749.

24 T. R. Simmons, G. Berggren, M. Bacchi, M. Fontecave and V. Artero, *Coord. Chem. Rev.*, 2014, **270**, 127–150.

25 E. J. Reijerse, C. C. Pham, V. Pelmenschikov, R. Gilbert-Wilson, A. Adamska-Venkatesh, J. F. Siebel, L. B. Gee, Y. Yoda, K. Tamasaku, W. Lubitz, T. B. Rauchfuss and S. P. Cramer, *J. Am. Chem. Soc.*, 2017, **139**, 4306–4309.

26 A. Silakov, B. Wenk, E. Reijerse and W. Lubitz, *Phys. Chem. Chem. Phys.*, 2009, **11**, 6592–6599.

27 M. Bourrez, R. Steinmetz and F. Gloaguen, *Inorg. Chem.*, 2014, **53**, 10667–10673.

28 H. Li and T. B. Rauchfuss, *J. Am. Chem. Soc.*, 2002, **124**, 726–727.

29 J. A. Wright, L. Webster, A. Jablonskytė, P. M. Woi, S. K. Ibrahim and C. J. Pickett, *Faraday Discuss.*, 2011, **148**, 359.

30 J. L. Stanley, Z. M. Heiden, T. B. Rauchfuss, S. R. Wilson, L. De Gioia and G. Zampella, *Organometallics*, 2008, **27**, 119–125.

31 S. J. Borg, T. Behrsing, S. P. Best, M. Razavet, X. Liu and C. J. Pickett, *J. Am. Chem. Soc.*, 2004, **126**, 16988–16999.

32 S. H. Wang, A. Aster, M. Mirmohades, R. Lomoth and L. Hammarström, *Inorg. Chem.*, 2018, **57**, 768–776.

33 M. Mirmohades, S. Pullen, M. Stein, S. Maji, S. Ott, L. Hammarström and R. Lomoth, *J. Am. Chem. Soc.*, 2014, **136**, 17366–17369.

34 K. Izutsu, *Acid-Base Dissociation Constants in Dipolar Aprotic Solvents*, Blackwell, Oxford, 1990.

35 S. Tschierlei, S. Ott and R. Lomoth, *Energy Environ. Sci.*, 2011, **4**, 2340–2352.

36 E. S. Rountree and J. L. Dempsey, *Inorg. Chem.*, 2016, **55**, 5079–5087.

37 G. Eilers, L. Schwartz, M. Stein, G. Zampella, L. de Gioia, S. Ott and R. Lomoth, *Chem.–Eur. J.*, 2007, **13**, 7075–7084.

38 C. M. Klug, A. J. P. Cardenas, R. M. Bullock, M. O'Hagan and E. S. Wiedner, *ACS Catal.*, 2018, **8**, 3286–3296.

39 S. Löscher, L. Schwartz, M. Stein, S. Ott and M. Haumann, *Inorg. Chem.*, 2007, **46**, 11094–11105.